RECONNECTION IN SHEARED MAGNETIC FIELDS IN SPACE AND ASTROPHYSICS

James F. Drake
Laboratory for Plasma and Fusion Energy Studies
University of Maryland
College Park, Maryland 20742

ABSTRACT

The current theoretical understanding of the linear and nonlinear evolution of resistive tearing instabilities in sheared magnetic fields is reviewed. The physical mechanisms underlying this instability are emphasized. Some of the problems which are encountered in developing a model of magnetic energy dissipation in coronal loops are discussed and possible solutions are suggested.

I. INTRODUCTION

The conversion of magnetic to particle energy is a fundamental process which underlies such diverse phenomena in nature as disruptions in laboratory plasmas,[1] magnetic substorms in the magnetosphere of the earth,[2] and solar flares.[3] The development of theoretical models of this energy conversion process is therefore of central importance to our understanding of these basic phenomena.

The most simple models of magnetic energy conversion are based on a slab equilibrium such as that shown in Fig. 1. A plasma carrying a current $J_{z0}(x)$ generates the magnetic field $B_{y0}(x)$. When a uniform guide field $B_{z0} \gg B_{y0}$ is included in the configuration the equilibrium is unchanged but the magnetic field rotates through a finite angle as the region of current carrying plasma is crossed. For $B_{z0} = 0$ the magnetic field simply reverses. Only the former case, that of a sheared magnetic field, is considered in this paper.

When collisions are included in this 1-D equilibrium, the resistive diffusion of the magnetic field B_{y0} dissipates both magnetic energy and magnetic flux and the flux annihilation velocity V_B is given by a/τ_r, where $\tau_r = 4\pi a^2/\eta c^2$ is the resistive diffusion time based on the resistivity η and equilibrium scale size "a". In most applications the resistive diffusion time is far too long to explain the observed energy release time scales.

Faster rates of magnetic energy dissipation can be achieved by considering perturbations of the equilibrium in Fig. 1 which change the topology of the magnetic field by forming one or more x-points as shown in Figs. 2 and 3a. In Fig. 2 the plasma and magnetic field at $x = \pm\infty$ flow toward a single x-line at $x = 0$ as indicated by the short arrows. The inflowing magnetic field reconnects in the vicinity of the x-line and flows out at $y = \pm\infty$. In Fig. 3a the magnetic field reconnects to form a periodic set of x and 0-points with a flow pattern indicated by the thin arrows. In both configurations the flow is driven by the release in the tension of the reconnecting magnetic field, which will be discussed in more detail later.

While in the case of magnetic dissipation in the one-dimensional model, only one time scale, τ_r, entered the problem, the bending of the magnetic field in the x-y plane in Figs. 2 and 3 brings in a second fundamental time scale, the shear Alfvén time, $\tau_{Ay} = a/c_{Ay}$, where $c_{Ay} = (B_{y0}^2/4\pi m_i n)^{1/2}$ is the Alfvén velocity associated with the magnetic field B_{y0}. The ratio of these two times, the Lundquist number $S \equiv \tau_r/\tau_{Ay}$, is a large parameter in high temperature plasma. The existence of this second time scale implies that the characteristic time for magnetic energy dissipation can be a hybrid of τ_r and τ_{Ay} which can be much shorter than τ_r. Note that the compressional Alfvén time $\tau_{Az} = a/c_{Az} \ll \tau_{Ay}$ does not enter the problem because the large B_{z0} field contains no free energy and is simply convected with the fluid.

A number of steady state models of reconnection have been proposed which are based on the single x-line configuration shown in Fig. 2. Vasyliunas[4] has discussed these models in detail so we only briefly mention some essential features of these theories. In the Sweet-Parker[5] model magnetic reconnection takes place in an elongated layer (the region where resistivity is important) of width $\Delta x \sim a/S^{1/2}$ in the x direction and the system size in the y direction. The outflow velocity is the Alfvén speed c_{Ay} and the merging velocity V is given by

$$V/c_{Ay} \sim S^{-1/2} ,$$

so that the time scale for dissipation of magnetic energy is of order $(\tau_r/\tau_{Ay})^{1/2}$. In Petschek's[6] model the reconnection region is much smaller, scaling as $\Delta x \sim aS^{-1}\ln S$ and $\Delta y \sim S^{-1}\ln^2 S$ in the x and y directions, respectively. The outflow velocity is again the Alfvén speed with the merging velocity

$$V/c_{Ay} \sim (\ln S)^{-1} ,$$

much larger than the Sweet-Parker rate. In Petschek's model a set of slow shocks form outside the resistive region along the separatrices in Fig. 2. These slow shocks link the magnetic fields and flows within the outflow region to those in the inflow region. The time development of these slow shocks has been observed in numerical simulations[7] in which the inflow velocity V in Fig. 2 is imposed as a boundary condition.

As emphasized very strongly by Vasyliunas, the Petschek solution actually represents an upper bound on the reconnection rate and therefore neither the steady reconnection models nor simulations of forced reconnection where the inflow velocity is imposed externally can answer the important question: what is the characteristic magnetic energy dissipation rate or time scale which is generated by the hydromagnetic forces within the current carrying plasma? In order to address this question it is necessary to include all the forces within the plasma which are driving the reconnection and follow the time development of the system from some appropriate initial conditions. Such a calculation essentially reduces to solving for the nonlinear development of the tearing instability (or reconnection driven by an ideal mode such as the kink) in the geometry of interest. In the remainder of this paper, the basic properties of the linear resistive tearing instability and our current understanding of the nonlinear behavior of these and related instabilities is discussed. Because of space limitations, the tearing instability in the collisionless and long mean-free path regimes is not discussed. The interested reader is referred to Refs. 8 and 9 for a discussion of the linear and nonlinear behavior of the instability in these limits.

II.   LINEAR TEARING INSTABILITY

The tearing instability is the mechanism by which a current carrying plasma spontaneously evolves to a lower magnetic energy state. The magnetic energy released goes into bulk plasma motion as shown in Fig. 3a and into the internal plasma energy by Joule heating. The resistive tearing instability is described by the one-fluid magnetohydrodynamic equations,

$$\rho d\underset{\sim}{v}/dt = \underset{\sim}{J} \times \underset{\sim}{B}/c - \nabla p \ , \tag{1}$$

$$dp/dt + (\gamma_s - 1) \ p\nabla\cdot\underset{\sim}{v} = (\gamma_s - 1)\eta J^2 \ , \tag{2}$$

$$\nabla \times \underset{\sim}{B} = 4\pi\underset{\sim}{J}/c \ , \tag{3}$$

$$\nabla \times \underset{\sim}{E} + c^{-1}\partial\underset{\sim}{B}/\partial t = 0 \ , \tag{4}$$

$$\eta\underset{\sim}{J} = \underset{\sim}{E} + \underset{\sim}{v} \times \underset{\sim}{B}/c \ , \tag{5}$$

$$\nabla\cdot\underset{\sim}{B} = 0 \ ; \qquad \nabla\cdot\underset{\sim}{J} = 0 \ ; \qquad d/dt = \partial/\partial t + \underset{\sim}{v}\cdot\nabla \ , \tag{6}$$

where the mass density ρ is taken to be a constant, γ_s is the ratio of specific heats and other notation is standard. The forces driving the tearing instability and the fundamental structure of the mode are the same in slab and cylindrical geometry. For simplicity, we therefore first discuss the instability in the slab geometry of Fig. 1 in detail and then extend the results to a cylinder.

The tearing mode is driven by the relaxation in the tension of the

reconnecting magnetic field lines. This can be easily shown by using Eqs. (1) and (3) to write the force density $\underset{\sim}{F}$ on the local magnetofluid as

$$\underset{\sim}{F} = - \nabla(p+B^2/8\pi) + \underset{\sim}{B} \cdot \nabla \underset{\sim}{B}/4\pi .$$

Since the time scale associated with the growth of magnetic islands is much longer than compressional Alfvén time τ_{Az}, the plasma flow shown in Fig. 3a is incompressible ($\nabla \cdot \underset{\sim}{v} = 0$). In this limit the gradient term in the force density does not contribute to the energetics of the tearing mode. The instability is driven only by the magnetic tension. The forces driving the instability are illustrated in Fig. 3a. The force density, given by the local magnetic tension, is shown by the thick arrows and the flow velocity by the thin arrows. In the region outside of the separatrix of the magnetic island the plasma flow opposes the magnetic force. In this region the flow stretches the magnetic field lines, locally increasing the magnetic energy. Within the magnetic island, however, the flow and magnetic forces are aligned so that it is the relaxation of the magnetic stress of the reconnecting field lines which drives the flow and the magnetic energy is reduced in this region. It is quite clear from Fig. 3a that in the absence of resistivity, so that reconnection of the magnetic field can not take place, all perturbations increase the magnetic energy so there is no instability. Moreover, to the extent that the resistivity in a high temperature plasma is small (S is large), the tearing instability is a slowly growing mode.

We now simplify the magnetohydrodynamic equations given in Eqs. (1)-(6) to study the tearing mode in more detail. For simplicity we treat the case where $\partial/\partial z = 0$. In the low frequency limit $\partial/\partial t \ll \tau_{Az}^{-1}$, the plasma motion is nearly incompressible and the velocity can be represented by the stream function ϕ as

$$\underset{\sim}{v} = \hat{z} \times \nabla\phi . \tag{7}$$

An equation for the stream function is obtained by taking the curl of the momentum equation [Eq. (1)] and then taking the dot product with the unit vector z,

$$\rho d(\nabla^2 \phi)/dt = c^{-1} \underset{\sim}{B} \cdot \nabla J_z . \tag{8}$$

The magnetic field can similarly be expressed in terms of the $\hat{z}$ component of the vector potential as

$$\underset{\sim}{B} = B_{z0}\hat{z} - \hat{z} \times \nabla A_z , \tag{9}$$

and an equation for A_z follows from the $\hat{z}$ component of Eq. (3),

$$\nabla^2 A_z = - 4\pi J_z/c . \tag{10}$$

Since $\partial/\partial z = 0$, the vector potential A_z is also a flux function,

$\underset{\sim}{B} \cdot \nabla A_z = 0$, so that the flux surfaces are surfaces of constant A_z. From the z component of Ohm's law in Eq. (5), we obtain an equation for J_z,

$$\eta J_z = E_z - \underset{\sim}{B} \cdot \nabla \phi / c \ . \tag{11}$$

The electric field $E_z = - c^{-1} \partial A_z / \partial t$ follows from Eqs. (9) and (4), so that (11) becomes

$$\eta J_z = - c^{-1} (\partial A_z / \partial t + \underset{\sim}{B} \cdot \nabla \phi) \ . \tag{12}$$

Equations (6)-(10) and (12) provide a complete set of equations for both the linear and nonlinear tearing mode. In the incompressible limit considered here neither the pressure p nor B_{z0} enter the equations for the tearing mode. Of course, when $B_{z0} = 0$, the electrons and ions are demagnetized near x = 0 and the fluid equations can not be used to describe the plasma dynamics. The resistivity has been taken to be constant in time in Eq. (12) so that neither the rippling[10,11] nor the thermal instabilities[12,13] are described by these equations.

In the limit of $B_{z0} \gg B_{y0}$, the $\hat{z}$ direction is nearly aligned along the magnetic field, $A_z \simeq A_\parallel$, $J_z \simeq J_\parallel$, and Eq. (12) can be interpreted as the parallel Ohm's law,

$$\eta J_\parallel = E_\parallel = - c^{-1} (\partial A_\parallel / \partial t + \underset{\sim}{B} \cdot \nabla \phi) \ , \tag{13}$$

where the subscript $\parallel$ denotes the component along $\underset{\sim}{B}$. The stream function ϕ is now the electrostatic potential and the flow in Eq. (7) is simply given by the $\underset{\sim}{E} \times \underset{\sim}{B}$ drift associated with this potential. In the two fluid description of the tearing mode in this limit, Eq. (8) is the charge neutrality condition $n_i = n_e$ where n_i on the left side of Eq. (8) is the divergence of the ion polarization drift and the right side of (8) results from the parallel bunching of electrons.[8]

To study the linear tearing instability, we linearize the equations assuming all perturbed quantities vary as $\exp(\gamma t + i k_y y)$. The coupled second order equations for $\widetilde{A}_z$ and $\widetilde{\phi}$ are

$$\nabla^2 \widetilde{A}_z = - 4\pi \widetilde{J}_z / c \ , \tag{14}$$

$$\gamma \nabla^2 \widetilde{\phi} = i \underset{\sim}{k} \cdot \underset{\sim}{B} \widetilde{J}_z / c + i k_y \widetilde{A}_z J'_{z0} / c \ , \tag{15}$$

$$\eta \widetilde{J}_z = \widetilde{E}_\parallel = - (\gamma \widetilde{A}_z + i \underset{\sim}{k} \cdot \underset{\sim}{B} \widetilde{\phi}) / c \ , \tag{16}$$

where the prime denotes d/dx. Because of the x dependence of $\underset{\sim}{k} \cdot \underset{\sim}{B} = k_y B_{y0}(x)$ and $J_{z0}(x)$, these equations must be solved as an eigenvalue problem subject to the boundary conditions $\widetilde{\phi}, \widetilde{A}_z \to 0$ as $|x| \to \infty$. Further insight into the nature of the tearing mode can be gained by constructing an energy integral from Eqs. (14)-(16),

$$\frac{\partial}{\partial t} \int d\underset{\sim}{x} \; [\frac{1}{2} \rho |\nabla \tilde{\phi}|^2 + \frac{1}{8\pi} |\nabla \tilde{A}_z|^2 + \frac{1}{8\pi} \frac{B''_{y0}}{B_{y0}} |\tilde{A}_z|^2]$$

$$= - \int d\underset{\sim}{x} \eta \tilde{J}_z (\tilde{J}_z + \frac{J'_z}{B_{y0}} \tilde{A}_z) \; . \tag{17}$$

The first term on the left side of this equation is the flow kinetic energy, the second two terms combine to give the total change in magnetic energy, while the resistive term is the rate of dissipation of energy by Joule heating. To have instability we require that the magnetic energy decrease or[14]

$$\delta W_B = \frac{1}{8\pi} \int d\underset{\sim}{x} (|\nabla \tilde{A}_z|^2 + \frac{B''_{y0}}{B_{y0}} |\tilde{A}_z|^2) < 0 \; . \tag{18}$$

The first term in the integral, which is positive and therefore stabilizing, is the square of the first order fields, $\tilde{B}^{(1)} \cdot \tilde{B}^{(1)}$, while the second comes from the second order field, $\tilde{B}_y^{(2)} B_{y0}$. For the equilibrium of Fig. 1, the second term is destabilizing (negative) and scales as $a^{-2} |\tilde{A}_z|^2$, where "a" is the characteristic length of the equilibrium magnetic field, while the first is stabilizing and scales as $k_y^{-2} |\tilde{A}|^2$. For instability we therefore require $k_y a < 1$ so that the tearing instability is inherently a long wavelength phenomena. Note also that $B''_{y0} = J'_{z0}$ so that the instability is driven by the gradient of the equilibrium current.

We now return to discuss the solutions to Eqs. (14)-(16). In high temperature plasma where $S \gg 1$ the resistivity η in Eq. (16) can be neglected throughout most of the plasma so that $\hat{E}_{\parallel} = 0$, i.e., the parallel induction and electrostatic fields balance. The cancellation between these terms occurs because of the high electron mobility along $\underset{\sim}{B}$. The bunching of electrons parallel to $\underset{\sim}{B}$ driven by the induction field produces an electrostatic field which effectively shorts out the induction field. The condition $\tilde{E}_{\parallel} = 0$ can be rewritten as

$$\partial \tilde{A}_z / \partial t + \tilde{v}_x \partial A_z / \partial x = 0 \; , \tag{19}$$

so that the rate of change of flux in the frame of the moving fluid is zero. In the "ideal" region the plasma and flux are frozen together. The inertia term on the left-hand side of Eq. (15) can be neglected in the ideal region so the two terms on the right side of the equation balance and

$$\tilde{J}_z = - (\tilde{A}_z / B_{y0}) J'_{z0} \; . \tag{20}$$

The plasma displacement Δx can be calculated using Eq. (19) as $\Delta x = - \tilde{A}_z / B_{y0}$. Thus, the perturbed current in the ideal region simply results from the displacement of the equilibrium current J_{z0}. Equations

(14) and (20) yield a single second order equation for $\widetilde{A}_z$ valid in the ideal region,

$$\nabla^2 \widetilde{A}_z - (B_{y0}''/B_{y0})\widetilde{A}_z = 0 \ . \tag{21}$$

The parallel induction and electrostatic fields balance everywhere except where the parallel electrostatic field is zero in the vicinity of $\underset{\sim}{k} \cdot \underset{\sim}{B} = 0$ [see Eq. (16)], or for the equilibrium of Fig. 1 at $x = 0$. In this region $\widetilde{E}_\parallel \neq 0$ and since η is small a large parallel current $\widetilde{J}_z$ is driven. For an ideal mode, where η is taken to be strictly zero, $\widetilde{A}_z(x=0) = 0$ and since $\widetilde{B}_x = ik_y\widetilde{A}_z = 0$, no magnetic island is formed. However, for a resistive mode such as the tearing mode, this constraint does not apply and $\widetilde{B}_x(x=0) \neq 0$ allowing a magnetic island to form as in Fig. 3a. Because η is small, the region Δ around $x = 0$ where $\widetilde{E}_\parallel \neq 0$ is also small ($\Delta/a \ll 1$) so that Eq. (21) for $\widetilde{A}_z$ is valid throughout most of the plasma.

A typical solution of the ideal equation for $\widetilde{A}_z$ is shown in Fig. 4a for a mode with $k_y a < 1$. The slope of $\widetilde{A}_z$ is discontinuous across $x = 0$ where the ideal equation for $\widetilde{A}_z$ breaks down. In the region $x \sim \Delta$ resistivity must be retained in the equation for $\widetilde{A}_z$ and the solutions of this equation must be matched to the ideal solutions so that the complete solution for $\widetilde{A}_z$ is continuous everywhere. Nevertheless, the ideal solution can be characterized by the discontinuity in the slope of $\widetilde{A}_z$ at $x = 0$ as measured by the quantity[10]

$$\Delta' = [\partial\widetilde{A}_z(x=0^+)/\partial x - \partial\widetilde{A}_z(x=0^-)/\partial x]/\widetilde{A}_z(0) \ . \tag{22}$$

For the Harris equilibrium, $B_{y0} = B_{y00}\tanh(x/a)$, the parameter Δ' can be calculated analytically as

$$\Delta'a = 2(1 - k_y^2 a^2)/|k_y|a \ . \tag{23}$$

The parameter Δ' is related to the magnetic energy released by the tearing mode. This relation can be derived by multiplying Eq. (21) by $\widetilde{A}_z$ and integrating over the region $|x| > \Delta$. After an integration by parts, we find

$$\Delta' = - 8\pi\delta W_B/\int dy |\widetilde{A}_z(x=0)|^2 \ . \tag{24}$$

The tearing mode should be unstable for $\delta W_B < 0$ or $\Delta' > 0$.

The equations governing the resistive region $|x| \sim \Delta \ll a, k_y^{-1}$ are obtained from Eqs. (14)-(16) by neglecting J_{z0}' in (15) and approximating $\nabla^2 \simeq \partial^2/\partial x^2$ and $\underset{\sim}{k} \cdot \underset{\sim}{B} = k_y B_{y0}' x$,

$$\widetilde{A}_z'' = (4\pi\gamma/\eta c^2)(\widetilde{A}_z + x\hat{\phi}/\Delta) \ , \tag{25}$$

$$\hat{\phi}'' = (x/\Delta^3)(\widetilde{A}_z + x\hat{\phi}/\Delta) \ , \tag{26}$$

$$\Delta/a = (\gamma\tau_{Ay}/Sk_y^2 a^2)^{1/4} ,\tag{27}$$

where Δ is the scale length of the resistive layer and $\hat{\phi} \equiv ik_y B_{0y}' \Delta\widetilde{\phi}/\gamma$. The equations describe the transition from $\widetilde{E}_\parallel = -\gamma\widetilde{A}_z/c$ at $x \lesseqgtr 0$ to $\widetilde{E}_\parallel \approx 0$ for $x \gg \Delta$ as illustrated in Fig. 4b. While the resistive layer equations can be solved exactly, in the limit $4\pi\gamma\Delta^2/\eta c^2 \ll 1$, the flux perturbation $\widetilde{A}_z$ can readily diffuse across the resistive layer Δ during the growth time γ^{-1} of the mode so that $\widetilde{A}_z(x)$ is nearly constant in the resistive region and can be approximated by $\widetilde{A}_z(0)$ on the right side of Eqs. (25) and (26). This is the widely invoked "constant ψ" approximation.[10] Equation (26) can now be readily inverted to obtain ϕ and Eq. (25) can then be integrated to obtain the jump in $\partial\widetilde{A}_z/\partial x$ across the resistive layer. Matching this jump with that obtained from the ideal solution in (23), we obtain the growth rate of the resistive tearing mode, [10]

$$\gamma\tau_{Ay} = S^{-3/5}[(1 - k_y^2 a^2)\Gamma(1/4)/\pi\Gamma(3/4)]^{4/5}(k_y a)^{-2/5}\tag{28}$$

For $k_y a \lesssim 1$, $\Delta/a \sim S^{-2/5} \ll 1$ so the resistive layer is indeed small. The expression for the growth rate in (28) implies that the fastest growing modes are those with $k_y a \ll 1$. The "constant ψ" approximation breaks down for $k_y a$ too small since both Δ and γ increase with decreasing k_y. The fastest growing modes are those with $k_y a \sim S^{-1/4}$, for which $4\pi\gamma\Delta^2/\eta c^2 \sim 1$, i.e., the growth time and diffusion time across the resistive layer are comparable.[15] In practical applications where S is very large, however, the finite geometry of the system often prevents $k_y a$ from being as small as $S^{-1/4}$.

In deriving the dispersion relation in Eq. (28), we assumed $\partial/\partial z = ik_z = 0$ so that $\underset{\sim}{k}\cdot\underset{\sim}{B} = 0$ at $x = 0$ and the magnetic island forms symmetrically in this region as shown in Fig. 3a. When $k_z \neq 0$, the linear tearing mode equations in (14)-(16) are still valid as long as $B_{z0} \gg B_{y0}$. Resistivity is again important where

$$\underset{\sim}{k}\cdot\underset{\sim}{B} = k_y B_{y0}(x) + k_z B_{z0} = 0,$$

which is now at $x = x_0 \neq 0$. The magnetic islands form around x_0 and are driven by the reconnection of the magnetic flux corresponding the component of $\underset{\sim}{B}$ along $\underset{\sim}{k}$, which reverses sign at $\underset{\sim}{k}\cdot\underset{\sim}{B} = 0$. The calculation of the growth rate of the nonsymmetric islands is basically unchanged from that presented for the symmetric case. The growth rates are generally smaller than when $k_z = 0$ because Δ' is reduced.

The location and size of the magnetic islands formed can be calculated by constructing the flux function defined by

$$\underset{\sim}{B}\cdot\nabla\psi = B_{z0}\partial\psi/\partial z - \hat{z} \times \nabla A_z\cdot\nabla\psi = 0 .\tag{29}$$

Such a function ψ can generally only be constructed for 2-D problems in which $\psi = \psi(x,y+pz)$, where p is a constant. For this case $\partial/\partial z = p\,\partial/\partial y$ and

$$\psi = pB_{z0}x - A_z(x,y+pz) \ . \tag{30}$$

The islands form where the equilibrium flux function, ψ_0, has an extremum, or

$$\partial\psi_0/\partial x = [pB_{z0}x - A_{z0}(x)]' = (k_zB_{z0} + k_yB_{y0})/k_y = 0 \ , \tag{31}$$

i.e., where $\underset{\sim}{k}\cdot\underset{\sim}{B} = 0$. Note that ψ_0 is the flux associated with the component of $\underset{\sim}{B}$ along $\underset{\sim}{k}$. The island size is calculated by including the perturbation $\widetilde{A}_z = \widetilde{A}_z(x)\cos k_y(y+pz)$ in Eq. (30) and expanding x around x_0,

$$\psi = B'_{y0}(x-x_0)^2/2 + \widetilde{A}_z(x_0)\cos[k_y(y+pz)] \ . \tag{32}$$

Since ψ is a constant along a given magnetic field line, the structure of the magnetic island can be mapped out by calculating the constant ψ surfaces. The island width w is simply

$$w = [2\widetilde{A}_z(x_0)/|B''_{y0}|]^{1/2} \ . \tag{33}$$

Before discussing the nonlinear behavior of the tearing instability, we will complete our description of the linear mode by discussing the case of a cylindrical equilibrium. Consider a plasma carrying a current $J_{z0}(r)$ which produces a poloidal field $B_{\theta0}(r)$ and is periodic in z over the length L. For simplicity, we again consider the limit of a large axial magnetic field $B_{z0} \gg B_{\theta0}$. The pitch of the magnetic field line is measured by the quantity

$$q = 2\pi rB_{z0}/LB_{\theta0}(r) \ . \tag{34}$$

The parameter q increases monotonically with increasing r for current profiles peaked around r = 0. As in the slab geometry, a flux function can be defined for the 2-D case where $\psi = \psi(r,\theta + 2\pi pz/L)$. The flux function can be easily calculated as

$$\psi = pB_{z0}\pi r^2/2 - A_z(r,\theta + 2\pi pz/L) \ ,$$

and again reconnection can occur where $\underset{\sim}{k}\cdot\underset{\sim}{B} = 0$. In a cylinder periodicity in θ and z requires $k_\theta = m/r$ and $k_z = -2\pi m/L$, where m and n are integers, so that

$$\underset{\sim}{k}\cdot\underset{\sim}{B} = [m-nq(r)]B_{\theta0}(r)/r \ , \tag{35}$$

and p = - m/n. Tearing modes can therefore only form at discrete rational surfaces r_0 where $q(r_0) = m/n$.

The essential physics of tearing in a cylinder is unchanged from that in slab geometry and in particular the linearized Eqs. (14)-(16) are also valid for the cylinder if $k_y J_{z0}' \rightarrow k_\theta \partial J_{z0}/\partial r$ and k_z^2 is neglected compared with k_θ^2 in the ∇^2 operators. Because of geometrical effects, the magnetohydrodynamic driving energy Δ' is approximately an order of magnitude larger in the cylinder than in the slab.[16]

The most significant new feature in a cylinder is the existence of the m=1 kink mode.[17-19] For the slab tearing mode it was previously shown (Fig. 3) that the stretching of the magnetic field in the region outside of the magnetic island was stabilizing. This argument does not apply to the kink mode as can be seen in Fig. 5. The inner region of the plasma, where $q < n^{-1}$ is displaced uniformly while the outer region, where $q > n^{-1}$, remains stationary. Large poloidal flows emanating from the region of the x-line enable the flow to remain nearly incompressible. A uniform displacement of the plasma does not cause any distortion of the magnetic field lines so there is no restoring force from magnetic tension as in the slab or as with cylindrical modes with m≠1. Indeed, the magnetic forces in the ideal region are destabilizing where $q(r) < n^{-1}$ and the kink mode is unstable when $q(0) < n^{-1}$ even in the ideal limit.[17,18]

A detailed calculation of the stability of the kink tearing mode has been carried out previously[19] and we do not repeat the details here. The procedure is basically the same as that used to calculate the growth rate of tearing modes in slab geometry. The ideal equations are solved away from the rational surface and the discontinuity in the ideal solutions across the rational surface is bridged with the solutions of the resistive equations similar to those in Eqs. (25) and (26). The result is that the growth rate of the kink-tearing mode is the larger of the ideal,[18]

$$\gamma\tau_{A\theta} = \frac{\pi n}{|B_\theta^2 q'|_{r_0}} \left(\frac{2\pi}{L}\right)^2 \int_0^{r_0} dr B_\theta^2 (1 - nq)(3nq + 1)$$

$$\sim \left(2\pi r_0/L\right)^2 , \tag{36}$$

and resistive,

$$\gamma\tau_{A\theta} = (\tau_{A\theta}/\tau_r)^{1/3}(q'r_0 n)^{-4/3} , \tag{37}$$

growth rates where $\tau_{A\theta}$ is Alfvén time based on $B_\theta (r_0)$ and the length r_0 and τ_r is the resistive time based on r_0. It should be emphasized that the "constant ψ" approximation does not apply to the m=1 mode. In fact, the dispersion relation of the kink tearing mode in Eq. (37) can be expressed as

$$4\pi\gamma\Delta^2/\eta c^2 \sim 1 , \tag{38}$$

where

$$(\Delta/r_0) = (\gamma\tau_{A\theta}^2/\tau_r q'^2 r_0^2)^{1/4} \tag{39}$$

is the resistive layer thickness [from Eqs. (15) and (16)]. The growth
time of the resistive kink mode is therefore given by the flux diffusion
time across the resistive layer.

When the kink mode is discussed in the literature, the ideal
external kink, in which $q(r) < n^{-1}$ throughout the entire plasma and the
rational surface falls in the vacuum region,[12] and the ideal internal
kink in which $q(0) < n^{-1}$ but the rational surface lies within the
plasma,[17,18] are often treated as entirely separate instabilities. The
growth rate of the external kink is of order $\tau_{A\theta}^{-1}$, which is much larger
than that of the internal mode given in Eq. (36). A vacuum can be
considered as the limit of a very resistive plasma, so when resistivity
is included there is a continuous transition between these two modes.
When the rational surface falls in the region of high conductivity, the
growth rate is given in Eq. (36). As the rational surface moves towards
larger r, where η is larger, the growth rate increases until $\tau_{A\theta} \sim \tau_r$
when $\gamma \sim \tau_{A\theta}^{-1}$. At this point, of course, Δ is no longer small so that
the matching procedure which leads to the growth rates in Eqs. (36) and
(37) is invalid and inertia must be retained through the entire plasma.

An important point which is often overlooked in invoking the
tearing mode to explain physical phenomena is that the linear treatment
of this instability mode is valid only when the width of the magnetic
island w is smaller than the resistive layer thickness Δ. When $w \sim \Delta$,
the island structure strongly modifies the magnetic geometry of the
dissipation region. Since $\Delta \ll a$, for a high temperature plasma the
linear theory only applies when w is extremely small. As a consequence,
the linear growth time of the mode has no relation with the time
required to dissipate a significant fraction of the magnetic free energy
in a current carrying plasma. The nonlinear development of the tearing
mode must be studied to address this problem.

III. NONLINEAR TEARING INSTABILITIES

When the width w of the magnetic island of the tearing mode becomes
comparable to the width of dissipation region Δ, the magnetic structure
of the dissipation region is strongly modified. Since the growth rate
of the tearing mode is sensitive to the plasma dynamics in this
resistive region, the evolution of the mode should be strongly affected
once
$w > \Delta$.

For simplicity, we consider the slab geometry tearing mode of
Fig. 3 with $\partial/\partial z = 0$. Equations (7)-(10) and (12) describe the
nonlinear behavior of the 2-D structure of the mode in the x-y plane.
When $\Delta < w \ll a$, the dominant nonlinear behavior of the tearing mode is

produced by the $\underset{\sim}{B}\cdot\nabla$ operators in Eqs. (8) and (12) in the resistive
layer. We therefore first focus on this region where $\nabla^2 \approx \partial^2/\partial x^2$ and
equilibrium currents can be neglected. In the linear phase the left and
right sides of Eq. (8) are comparable. When the island width w exceeds
the tearing width the scale size of the resistive region increases so
that the inertia term scales as $\rho\gamma\,\tilde{\phi}/w^2$ and is therefore reduced. By
contrast, the right side of (8) should scale as $c^{-1}B'_{y0}w\tilde{J}_z$, which
increases with w. To lowest order, the inertia in Eq. (8) can therefore
be neglected, leaving[20]

$$\underset{\sim}{B}\cdot\nabla\tilde{J}_z = 0 \ , \tag{40}$$

where $\underset{\sim}{B} = \underset{\sim}{B}_0 + \underset{\sim}{\tilde{B}}$ is the total field. Nonlinearly, $\tilde{J}_z$ is a constant
along the magnetic field line and Eq. (12) can therefore be averaged
over a field line,

$$\eta\tilde{J}_z = \eta\langle\tilde{J}_z\rangle = -c^{-1}\langle\partial\tilde{A}_z/\partial t\rangle \ , \tag{41}$$

where $\langle\ \rangle$ denotes the average over one period of the tearing mode and
$\langle\underset{\sim}{B}\cdot\nabla\tilde{\phi}\rangle = 0$ since $\tilde{\phi}$ is periodic. Combining Eq. (41) with Ampere's law,
we obtain a nonlinear equation for $\tilde{A}_z$,

$$\tilde{A}''_z = -(4\pi/\eta c^2)\langle\partial\tilde{A}_z/\partial t\rangle \ . \tag{42}$$

Note that although $\tilde{\phi}$ does not appear in Eq. (42), $\tilde{\phi}$ is certainly not
negligible. In fact, the parallel bunching of electrons along $\underset{\sim}{B}$ by
$\partial\tilde{A}_z/\partial t$ produces the potential $\tilde{\phi}$ which forces $\tilde{E}_\parallel$ to be constant along $\underset{\sim}{B}$.
If we represent $\tilde{A}_z$ by a single harmonic $\cos k_y y$ and invoke the "constant
ψ" approximation, $\langle\partial\tilde{A}_z/\partial t\rangle \simeq (\partial\tilde{A}_z(0)/\partial t)\langle\cos k_y y\rangle$. It is easily seen
by comparing Figs. 3a and 3b that $\langle\cos k_y y\rangle \sim 1$ within the magnetic
island and is zero outside. Nonlinearly, the resistive layer width is
therefore given by the width of the magnetic island. Integrating Eq.
(42) across the island and matching to the outer ideal solution as in
the linear theory, we obtain the Rutherford expression for the rate of
increase of the magnetic island,[20]

$$d(w/a)/dt \sim \Delta'a/\tau_r \ . \tag{43}$$

The island width w grows linearly in time. Most significantly, w
becomes of order "a" on the resistive time scale τ_r so that the standard
tearing mode does not lead to a significant enhancement in the rate of
dissipation of magnetic flux. It is clear from Eq. (43) that inertia
does not play any role in the nonlinear growth of the mode. Consequent-
ly, the tearing mode simply represents the diffusive evolution of the
initial state to a more complex equilibrium. The expression for dw/dt
in (43) has been extended to include the quasilinear modification of the
equilibrium current profile, the result being that $\Delta'(0)$ in (43) is
replaced by $\Delta'(w)$, the discontinuity in the slope of the ideal solution
across the width of the island.[21] As can be seen in Fig. 4, $\Delta'(w) = 0$
for large enough w so the magnetic island eventually saturates. The
nonlinear evolution of slab modes with $k_z \neq 0$ and cylindrical modes is

basically unchanged from that of the symmetric slab mode.

The previous calculation of the nonlinear evolution of tearing modes does not apply to modes which violate the "constant ψ" approximation since the induction field $\partial \tilde{A}_z / \partial t$ may be very nonuniform within the magnetic island. Such modes include the very long wavelength tearing modes, the kink-tearing mode, the double tearing mode, and the coalescence instability. The double tearing mode occurs when $\underset{\sim}{k} \cdot \underset{\sim}{B} = 0$ at two locations which are close enough so that the flows associated with the reconnection at the two reversal layers drive each other.[22] This instability is stable when $\eta = 0$ but has a structure and growth rate which is similar to the kink-tearing mode for η not too small. The coalescence instability is driven by the attraction of the current filaments of adjacent magnetic islands in an existing island chain.[23] This is an ideal instability which, like the kink tearing mode, also drives reconnection when $\eta \neq 0$. The nonlinear behavior of the long wavelength and double tearing modes is currently not well understood.

The coalescence instability and the kink-tearing mode are the most likely candidates for producing fast reconnection since they are both ideally unstable and the flows are therefore strongly internally driven. Computer simulations of both of these instabilities have been performed and the qualitative features of the reconnection process are the same for both instabilities. During the initial ideal phase of the coalescence instability as shown in Fig. 6, two adjacent magnetic islands accelerate together and form a quasineutral layer at the location of the original x-point between the two.[24] Similarly in the cylinder the central region of current carrying plasma kinks and forms a quasineutral around the x-line shown in Fig. 5.[25,26] At this point the flow towards the quasineutral layer in both instabilities begins to force the reversed magnetic flux to reconnect. In both cases the reconnection velocity is roughly given by $v \sim a/(\tau_A \tau_r)^{1/2}$ and the vertical scale size of the quasineutral layer is independent of η, in agreement with the Sweet-Parker model. However, the dynamics of the process are much more complex than in the Sweet-Parker model. The neutral layer tends to break up into multiple magnetic islands and reconnection of the reversed flux occurs in bursts. It should also be emphasized that the boundaries in both simulations are far from the region of plasma flow and therefore do not inhibit the rate of reconnection. The clear conclusion from these simulations is that reconnection of magnetic flux does not typically occur at Petschek's rate but much slower. Of course, one can not eliminate the possibility that under some very special conditions faster reconnection may be possible.

The discussion of nonlinear tearing instabilities up to this point is valid for 2-D systems where the magnetohydrodynamic variables depend only on x and y+pz in the slab and r and $\theta - 2\pi m z/mL$ in a cylinder. While in the 2-D case the tearing mode grows rather slowly and then saturates in a rather benign manner, the evolution of the instability in 3-D can be much more violent. In 3-D simulations of the tearing mode in

a cylinder, the magnetic island of the m/n = 2/1 tearing mode can reach large amplitude, w/a ~ .4 - .5, when the initial current profile is fairly flat. When the magnetic island of the 2/1 mode approaches the q = 3/2 and 5/3 rational surfaces, the m/n = 3/2 and 5/3 modes are strongly destabilized. These modes subsequently destabilize even higher mode numbers, the entire process culminating in a broad spectrum of magnetic turbulence.[27] The destruction of the magnetic surfaces associated with the formation of the turbulent bath and the associated loss of particle and energy confinement has been correlated with the major disruptions in tokamak discharges. In detailed studies of the properties of this magnetic turbulence it has been shown that the dissipation of magnetic energy is dominated by the short wavelength component of the spectrum and that the effective resistivity, given by

$$\eta_{eff} = \eta_0 \int d\underline{x} \eta \tilde{J}^2 / \int d\underline{x} \eta J_0^2 \ ,$$

where η_0 is the spatial averaged value of $\eta(r)$, is nearly independent of η_0.[28]

The physical mechanism behind the destabilization of the short wavelength tearing modes has recently been investigated in some detail by examining the linear stability of a cylindrical equilibrium containing a large amplitude m/n = 2/1 magnetic island.[29] The 2/1 tearing mode grows by feeding off the current gradient in region r < r_0, where r_0 is the location of the 2/1 rational surface. As a consequence, the growth of the 2/1 mode actually steepens the current profile as shown in Fig. 7. The solid (dashed) line is the current profile after (before) the 2/1 mode reaches large amplitude. The arrows mark the position of inside and outside separatrices of the 2/1 magnetic island. In a 2-D simulation all modes have rational surfaces at the q=2 surface so no modes can be driven by the steep gradient in Fig. 7. In 3-D simulations other modes, such as the 3/2 and 5/3 modes, have rational surfaces in the region of large current gradient produced by the 2/1 mode. These modes are strongly destabilized with growth rates which are nearly independent of the resistivity.[29] It is also interesting to observe that this calculation of the onset of 3-D magnetic turbulence in the cylinder is quite similar to that of Poiseuille flow in fluids.[30]

IV. PROBLEMS IN UNDERSTANDING RECONNECTION IN SPACE AND ASTROPHYSICAL PLASMAS

Until recently, much of the linear and especially nonlinear work on tearing modes has been carried out for laboratory applications. Applications to space and astrophysical plasmas are complicated by generally more complex geometries and extremely large values of the Lundquist number $S = \tau_r/\tau_A$. As a specific example, we discuss efforts to understand magnetic energy dissipation in coronal loops. The structure and nonlinear evolution of collisionless and collisional tearing modes in the Earth's magnetosphere are also being studied.[31-33]

The dissipation of magnetic energy in coronal loops was proposed as a flare model a number of years ago.[34] Loops such as that shown in Fig. 8 are observed to be stable for many Alfvén times and then to release large amounts of energy ranging from 10^{28}-10^{30} ergs on a time scale of order 10^3 sec. The major radius of the loop is of order 10^9 cm and minor radius 10^8 cm. At the top of the loop in the corona (T ~ 100 ev, n_e ~ 10^9/cm^3, B ~ 200 G) $\tau_{A\theta}$ ~ 0.7 sec and τ_r ~ 1.3 x 10^{12} sec while at the base in the photosphere (T ~ 1 ev, n_e ~ 10^{13}/cm^3, n_n ~ 10^{16}/cm^3 and B ~ 10^3G) $\tau_{A\theta}$ ~ 14 sec with τ_r ~ 10^7 sec. The flare time scale is therefore intermediate between the Alfvén and resistive time scales.

The equilibrium of a loop such as shown in Fig. 8 is fully 3-D and therefore the equilibrium and ideal stability of the loop must be studied concurrently, i.e., no equilibrium can be found if the loop is unstable to an ideal MHD mode. The computation of an equilibrium is further complicated by the strong variation of the plasma parameters with altitude. It is not obvious that flux surfaces even exist for such a configuration. Sakurai has attempted to numerically solve for a 3-D force free equilibrium for a loop by specifying the normal magnetic flux at the photosphere.[35] He shows that the loop twists and expands upwards with increasing field aligned current. Greater resolution would improve these computations. Xue and Chen show than an axisymmetric equilibrium requires the pressure outside the loop to be greater than that inside to prevent the hoop force from causing the loop to expand.[36] A much more concerted effort will be required before the equilibrium of these loops is understood.

In the absence of a proper 3-D equilibrium the stability of coronal loops has been investigated by approximating the loop as a cylinder and applying boundary conditions at the ends to mock-up the effect of the photosphere. For ideal modes since $\tau_{A\theta}$(corona) << $\tau_{A\theta}$(photosphere), the appropriate boundary condition at the ends of the cylinder are $\underset{\sim}{\text{y}}$ = 0.[37] This constraint has a stabilizing influence on the ideal kink mode. For resistive modes this boundary condition does not seem appropriate. The growth time of the tearing mode based on photospheric parameters is ~10^5 sec, which is shorter than the ~10^7 sec. time scale for the corona.

Because of the very large Lundquist number, S ~ 10^{12}, for the corona, numerical calculations of the evolution of resistive modes with realistic parameters are not possible and the magnetic energy dissipation time scale for the corona must be extrapolated from the scaling of the dissipation rate in simulations at smaller values of S. The dissipation times of order τ_r for the standard tearing mode are far too long to explain the flare time scale. The Sweet-Parker scaling of reconnection rate for the kink-tearing mode or coalescence mode yields time scales of order 10^4 sec, which are much closer to the observed energy release times. Moreover, since the current density J near the neutral layer of the Sweet-Parker model scales as $\eta^{-1/2}$, which is very large for small η, nonclassical processes may limit J, thereby producing an anomalous resistivity and faster reconnection. In the standard
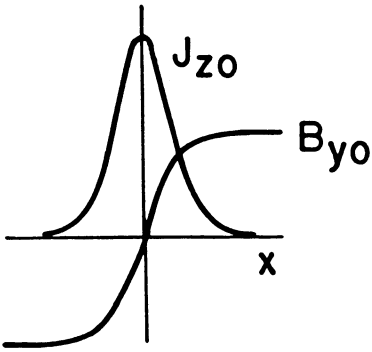
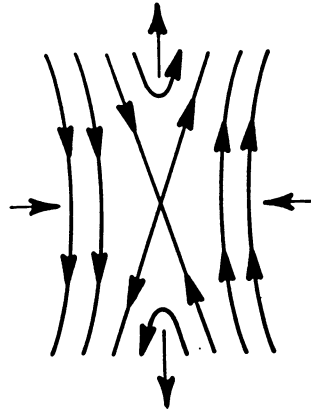Fig. 1   Slab equilibrium

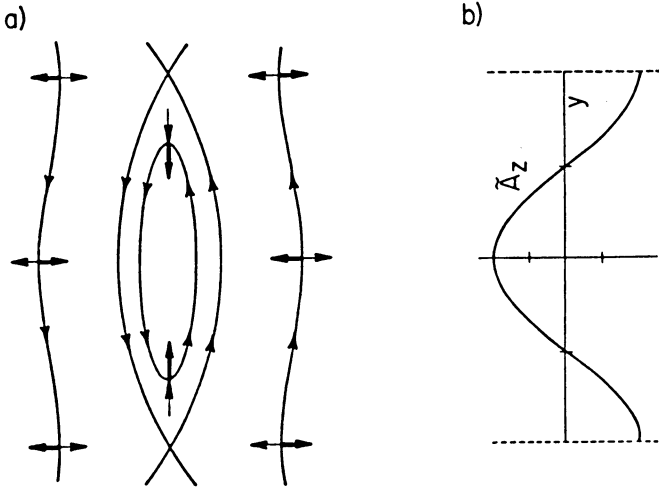Fig. 2   Reconnection at a
single x-line

Fig. 3   Reconnection at multiple x-lines:
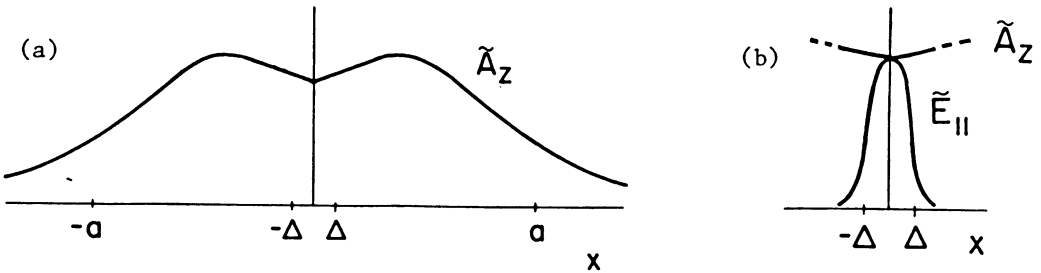the tearing instability

Fig. 4   Mode structure of tearing instability from ideal
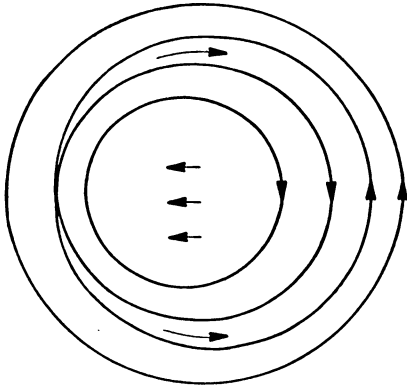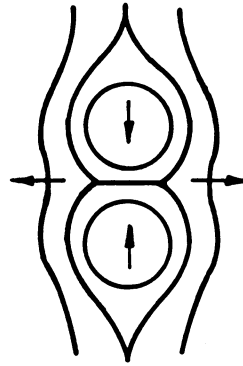equation (a) and resistive equations (b)

Fig. 5   Kink-tearing instability
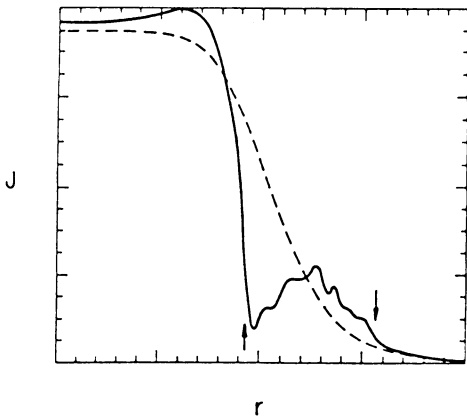
Fig. 6   Coalescence instability

Fig. 7   Current profile at t = 0
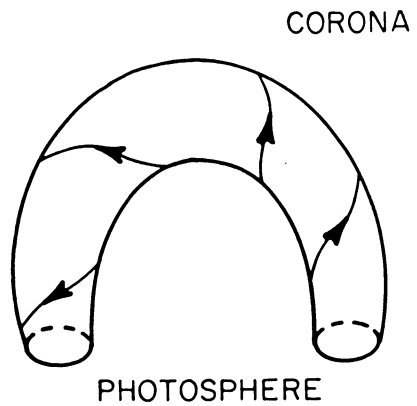(dashed) and after saturation
(solid) of m/n = 2/1 tearing
instability

Fig. 8   Magnetic loop in the
sun's corona

tearing mode where $J \propto \eta^0$ this would not occur.

The onset of the 3-D tearing mode turbulence is also fast enough to explain the observed energy release time scales. In such a scenario a small change in equilibrium parameters of the loop could cause an existing large amplitude tearing mode to exceed the rather sharp threshold for the onset of the secondary instabilities. The rapid growth of 3-D magnetic modes would rapidly dissipate the magnetic energy.

ACKNOWLEDGEMENTS

REFERENCES

1. N. R. Sauthoff, S. Von Goeler, and W. Stodiek, Nucl. Fusion 18, 1445 (1978).
2. S.-I. Akasofu, The Physics of Magnetospheric Substorms (D. Reidel, Dordrecht, Holland, 1977).
3. Solar Flares, edited by P. A. Sturrock (Colorado Assoc. Univ. Press, Denver, Co., 1980).
4. V. M. Vasyliunas, Rev. Geophys. Space Phys. 13, 303 (1975).
5. P. A. Sweet, in Proceedings of the Astronomical Union Symposium on Electromagnetic Phenomena in Cosmic Physics, No. 6, Stockholm, 1956 (unpublished) p. 123; E. N. Parker, Astrophys. J. Suppl. Ser. No. 77, 8, (1963).
6. H. E. Petschek, in AAS/NASA Symposium on the Physics of Solar Flares, edited by W. N. Hess (National Aeronautics and Space Administration, Washington, D.C., 1964) p. 425.
7. T. Sato and T. Hayashi, Phys. Fluids 22, 1189 (1979).
8. J. F. Drake and Y. C. Lee, Phys. Fluids 20, 1341 (1977).
9. J. F. Drake and Y. C. Lee, Phys. Rev. Lett. 39, 453 (1977).
10. H. P. Furth, J. Killeen, and M. N. Rosenbluth, Phys. Fluids 6, 459 (1963).
11. B. Coppi, Phys. Fluids 8, 2273 (1965); A. B. Hassam and J. F. Drake, Phys. Fluids 26, 133 (1983).
12. B. B. Kadomtsev, Reviews of Plasma Phys. (M. A. Leontovich, Ed., Consultants Bureau, N.Y., 1966) Vol. 2, p. 153.
13. G. Van Hoven, R. S. Steinolfson, and T. Tachi, Astrophys. J. 268, 860 (1983).
14. H. P. Furth, Nucl. Fusion Suppl. Pt. 1, 169 (1961).
15. R. S. Steinolfson and G. Van Hoven, Phys. Fluids 26, 117 (1983).
16. H. P. Furth, P. Rutherford, and H. Selberg, Phys. Fluids 16, 1054 (1973).

17. W. A. Newcomb, Ann. Phys. 10, 232 (1960).
18. M. N. Rosenbluth, R. Y. Dagazian, and P. H. Rutherford, Phys. Fluids 16, 1894 (1973).
19. B. Coppi, R. Galvao, R. Pellat, M. Rosenbluth, and P. Rutherford, Fiz. Plazmy 2, 961 (1976) [Sov. J. Plasma Phys. 2, 533 (1976)].
20. P. Rutherford, Phys. Fluids 16, 1903 (1973).
21. R. B. White, D. A. Monticello, M. N. Rosenbluth, and B. V. Waddell, Phys. Fluids 20, 800 (1977); R. B. White, D. A. Monticello, and M. N. Rosenbluth, Phys. Rev. Lett. 39, 1678 (1977).
22. P. L. Pritchett, Y. C. Lee, and J. F. Drake, Phys. Fluids 23, 1368 (1980).
23. J. M. Finn and P. K. Kaw, Phys. Fluids 20, 72 (1977); P. L. Pritchett and C. C. Wu, Phys. Fluids 22, 2140 (1979); A. Bondeson, Phys. Fluids 26, 1275 (1983).
24. D. Biskamp and H. Welter, Phys. Rev. Lett. 44, 1069 (1980).
25. W. Park, D. A. Monticello, R. B. White, and S. C. Jardin, Nucl. Fusion 20, 1181 (1980).
26. W. Park, D. A. Monticello, and R. B. White, Phys. Fluids 26, XXX (1983).
27. B. V. Waddell, B. Carreras, H. R. Hicks, and J. A. Holmes, Phys. Fluids 22, 896 (1979); Phys. Fluids 23, 1811 (1980).
28. D. Biskamp and H. Welter, in Plasma Physics and Controlled Nuclear Fusion Research (IAEA, Vienna, 1982) CN-41-TI.
29. R. G. Kleva, J. F. Drake, and A. Bondeson (submitted to Phys. Fluids); A. Bondeson (submitted to Phys. Fluids).
30. S. A. Orszag and A. T. Patera, Phys. Rev. Lett. 45, 989 (1980).
31. K. B. Quest and F. V. Coroniti, J. Geophys. Res. 86, 3289 (1982) and references therein.
32. J. G. Lyon, S. H. Brecht, J. D. Huba, J. A. Fedder, and P. J. Palmadesso, Phys. Rev. Lett. 46, 1038 (1981).
33. J. Birn (this meeting and references therein).
34. D. S. Spicer, Solar Phys. 53, 308 (1976); 71, 149 (1981).
35. T. Sakurai, Solar Phys. 69, 343 (1981).
36. M. L. Xue and J. Chen, Solar Phys. 84, 119 (1983).
37. A. W. Hood and E. R. Priest, Geophys. Astrophys. Fluids Dynamics 17, 297 (1981); G. Einaudi and G. Van Hoven, Solar Phys. 88, 163 (1983).

DISCUSSION

Wu: Did you consider gravitational effects in these studies? If not, would you care to comment on the effects of gravity on those coronal loops?

Drake: I have not considered the effect of gravity. Gravity is probably important. Otherwise how can one find an equilibrium in which the density at the bottom of the loop is 10^6 times larger than at the top?

Migliuolo: The density scale height becomes small near the photosphere. What are the effects of this inhomogeneity on the tearing mode?

Drake: The effects of density and temperature gradients along $\underset{\sim}{B}$ are completely unknown.

Birn: I would like to point out again that an asymmetry of the
current sheet in the direction parallel to it can also change the pos-
sible saturation of a tearing mode. Whereas in a plane current sheet
with periodic boundary conditions the location of the center of magnetic
islands is fixed in space, an asymmetric situation could produce moving
islands being pushed out from the diffusion region as shown in magneto-
tail simulations. This can lead to larger energization than possible in
a slab geometry with periodic boundary conditions.

Drake: I agree with your observation. In the magneto-tail, the
magnetic fields can act like a slingshot in ejecting plasma and flux away
from the earth.

I would also note, more generally, that the magnetic configuration may
strongly affect the nonlinear behavior of the reconnection process. It
is therefore important to carry out careful simulations of the particular
configuation of interest.

Kundu: I just wanted to alert you to the fact that there exist at
present values of temperature, density and magnetic field as a function
of height in a 3-D coronal loop. This is possible due to measurements
made in the radio (microwave) domain with the Very Large Array (VLA) at
several frequencies, which really explore different layers of the loop.
Also, there are soft x-ray measurements of coronal loops.

Drake: More detailed measurements will certainly help in building
models of energy dissipation in coronal loops.

Priest: What is the effect of the growth of the $m = 2$ mode on the
$m = 1$ mode and on the basic current profile?

Drake: The $m = 2$ mode does not strongly affect the $m = 1$ mode because
the rational surface of the $m = 1$ mode is rather far away from the mag-
netic island of the $m = 2$ mode.

The current profile before and after the $m = 2$ mode has reached large
amplitude is shown in Fig. 7 (more details can be found in Ref. 29). The
$m = 2$ mode basically dissipates most of the current in the vicinity of
its magnetic island, leaving an elliptically shaped current pedestal.

Sturrock: What conditions are required to lead to the mode inter-
action process investigated by Carreras and others? Are these conditions
likely to be met in coronal loops?

Drake: All that is required is a current profile which is somewhat
flat near the center with the $q = 2$ surface just outside of the steep
gradient (see dashed curve in Fig. 7). This current profile is not in
any sense unusual and therefore could very possibly be present in coronal
loops.

Van Hoven: i) I disagree with your statement that the tearing rate
is not anomalous. Tearing self-consistently generates a narrow enough
layer to be diffusive. However, it is anomalous on the global scale.
ii) I believe that very long wavelength modes can be added to your list
of $m = 1$ and double tearing modes as good nonlinear-release candidates.
We have done nonlinear calculations which show this.

Drake: The standard "constant ψ" tearing mode evolves to large
amplitude on the resistive time, and, is therefore not in any sense
anomalous.

The nonlinear behavior of very long wavelength modes is currently not
well understood. I think it is an important area of research.

Mahajan: If the minimum of current is formed in the plasma, then there is a possibility of exciting large growth rate double tearing modes discussed by Mahajan and Hazeltine, typically 10^3 times larger. Have those been considered?

Drake: The standard double tearing mode has been previously consider-ed by D. Spicer. The mode which you refer to has not been considered. I would emphasize again that the linear growth rate does not really give the time scale for the release of magnetic energy. It is essential to carry out a nonlinear calculation to find the energy dissipation rate.

Henriksen: Would there be any difference in the enhanced growth rates if the magnetic islands were formed by collision and coalescence of pre-viously existing flux tubes?

Drake: The coalescence instability is an ideal mode and the recon-nection time scales as $(\tau_r \tau_A)^{1/2}$, which is much faster than the standard tearing mode.

D. Smith: Van Hoven and one of his students showed that when you consider line tying, only the m = 1 mode is linearly unstable. How would this affect the possibility of 3-D magnetic turbulence?

Drake: As I have mentioned, the growth time of the tearing mode based on the parameters of the photosphere is actually shorter than the growth time based on the parameters of the corona. So it is not obvious to me that line tying boundary conditions at the photosphere are appropriate for resistive modes. Line tying conditions are appropriate for ideal modes.